Please cite this article in press as: Blackburn et al., Bi-allelic Alterations in *AEBP1* Lead to Defective Collagen Assembly and Connective Tissue Structure Resulting in a Variant of E..., The American Journal of Human Genetics (2018), https://doi.org/10.1016/j.ajhg.2018.02.018

REPORT

Bi-allelic Alterations in *AEBP1* Lead to Defective Collagen Assembly and Connective Tissue Structure Resulting in a Variant of Ehlers-Danlos Syndrome

Patrick R. Blackburn,[1,2,3,17] Zhi Xu,[4,17] Kathleen E. Tumelty,[5] Rose W. Zhao,[5] William J. Monis,[5] Kimberly G. Harris,[6] Jennifer M. Gass,[7] Margot A. Cousin,[2,3] Nicole J. Boczek,[1,2,3] Mario V. Mitkov,[8] Mark A. Cappel,[8] Clair A. Francomano,[4,9] Joseph E. Parisi,[1,10] Eric W. Klee,[1,2,3,11] Eissa Faqeih,[12] Fowzan S. Alkuraya,[13,14,15] Matthew D. Layne,[5] Nazli B. McDonnell,[4,16,*] and Paldeep S. Atwal[6,7,*]

AEBP1 encodes the aortic carboxypeptidase-like protein (ACLP) that associates with collagens in the extracellular matrix (ECM) and has several roles in development, tissue repair, and fibrosis. ACLP is expressed in bone, the vasculature, and dermal tissues and is involved in fibroblast proliferation and mesenchymal stem cell differentiation into collagen-producing cells. *Aebp1*$^{-/-}$ mice have abnormal, delayed wound repair correlating with defects in fibroblast proliferation. In this study, we describe four individuals from three unrelated families that presented with a unique constellation of clinical findings including joint laxity, redundant and hyperextensible skin, poor wound healing with abnormal scarring, osteoporosis, and other features reminiscent of Ehlers-Danlos syndrome (EDS). Analysis of skin biopsies revealed decreased dermal collagen with abnormal collagen fibrils that were ragged in appearance. Exome sequencing revealed compound heterozygous variants in *AEBP1* (c.1470delC [p.Asn490_Met495delins(40)] and c.1743C>A [p.Cys581*]) in the first individual, a homozygous variant (c.1320_1326del [p.Arg440Serfs*3]) in the second individual, and a homozygous splice site variant (c.1630+1G>A) in two siblings from the third family. We show that ACLP enhances collagen polymerization and binds to several fibrillar collagens via its discoidin domain. These studies support the conclusion that bi-allelic pathogenic variants in *AEBP1* are the cause of this autosomal-recessive EDS subtype.

Ehlers-Danlos syndrome (EDS) and EDS variants comprise a growing number of clinically heterogeneous connective tissue disorders with diverse molecular etiologies.[1–3] EDS is estimated to affect approximately 1 in every 5,000 individuals and is often caused by pathogenic variation in fibrillar collagen genes (*COL1A1* [MIM: 120150], *COL1A2* [MIM: 120160], *COL3A1* [MIM: 120180], *COL5A1* [MIM: 120215], *COL5A2* [MIM: 120190]), collagen-modifying proteins (*PLOD1* [MIM: 153454], *P4HA1* [MIM: 176710][4]), or processing enzymes (*ADAMTS2* [MIM: 604539]).[2] Several genes involved in the biosynthesis of proteoglycans (*CHST14* [MIM: 608429], *B4GALT7* [MIM: 604327], *B3GALT6* [MIM: 615291]), when mutated, result in EDS subtypes.[2] Pathogenic variants in other noncollagenous protein-coding genes, such as *TNXB* (MIM: 600985), *SLC39A13* (MIM: 608735), and *FKBP14* (MIM: 614505), also cause rare EDS subtypes suggesting that additional genes with diverse biological functions related to collagen biosynthesis and assembly may be contributory to disease in the EDS spectrum.[2] Together these known genes and their encoded proteins regulate the expression, assembly, homeostasis, and remodeling processes that are essential for the development and maintenance of the extracellular matrix (ECM).[2,5,6] Differences in ECM structure and composition in a variety of tissues throughout the body result in a broad spectrum of disease phenotypes in affected individuals.[1] Clinically, affected individuals present with connective tissue defects that may manifest as joint hypermobility, skin hyperextensibility and/or fragility, deficient wound healing, an increased risk of vascular rupture, and many other associated clinical features, and there may be considerable phenotypic overlap between individuals that carry distinct molecular diagnoses.[2] Recently, the International EDS Consortium proposed the 2017 International Classification for the Ehlers-Danlos Syndromes[7] with a new classification schema that recognizes 13 distinct subtypes and provides significant updates to the Villefranche nosology.[8] This new classification system outlines the major and minor criteria that may be associated with each subtype and emphasizes the importance of molecular confirmation for the diagnosis of individuals and incorporation of next-generation sequencing approaches for the

[1]Department of Laboratory Medicine and Pathology, Mayo Clinic, Rochester, MN 55905, USA; [2]Department of Health Sciences Research, Mayo Clinic, Rochester, MN 55905, USA; [3]Center for Individualized Medicine, Mayo Clinic, Rochester, MN 55905, USA; [4]Laboratory of Clinical Investigation, National Institute on Aging, NIH, Baltimore, MD 21224, USA; [5]Department of Biochemistry, Boston University School of Medicine, Boston, MA 02118, USA; [6]Department of Clinical Genomics, Mayo Clinic, Jacksonville, FL 32224, USA; [7]Center for Individualized Medicine, Mayo Clinic, Jacksonville, FL 32224, USA; [8]Department of Dermatology, Mayo Clinic, Jacksonville, FL 32224, USA; [9]Greater Baltimore Medical Center, Towson, MD 21204, USA; [10]Department of Neurology, Mayo Clinic, Rochester, MN 55905, USA; [11]Department of Clinical Genomics, Mayo Clinic, Rochester, MN 55905, USA; [12]Department of Pediatric Specialties, Children's Hospital, King Fahad Medical City, Riyadh 12231, Saudi Arabia; [13]Saudi Human Genome Project, King Abdulaziz City for Science and Technology, Riyadh 12371, Saudi Arabia; [14]Department of Genetics, King Faisal Specialist Hospital and Research Center, Riyadh 12713, Saudi Arabia; [15]King Abdullah University of Science and Technology (KAUST), Division of Biological and Environmental Sciences and Engineering (BESE), Thuwal 23955-6900, Saudi Arabia; [16]Veteran's Administration, Eastern Colorado Health System, Denver, CO 80220, USA
[17]These authors contributed equally to this work
*Correspondence: nazli.mcdonnell@va.gov (N.B.M.), paldeep.atwal@googlemail.com (P.S.A.)
https://doi.org/10.1016/j.ajhg.2018.02.018.

identification of novel EDS-associated genes. Importantly, in a significant proportion of suspected EDS-affected case subjects, no pathogenic variants in the known EDS genes are found. While our understanding of the molecular basis for the heritable connective tissue disorders has improved over the last few decades, the full extent and molecular underpinnings for several "unspecified" EDS-like conditions is the subject of intense ongoing study.[1,9]

The adipocyte enhancer binding protein 1 (*AEBP1* [MIM: 602981]) encodes a 1,158-amino acid secreted aortic carboxypeptidase-like protein (ACLP) that is associated with the extracellular matrix (ECM). ACLP consists of an N-terminal signal peptide, a lysine/proline/glutamic acid-rich motif, a discoidin domain, and a catalytically inactive metallocarboxypeptidase domain that shares ~40% similarity with carboxypeptidase E (*CPE* [MIM: 114855]).[10–13] ACLP is secreted by a number of different cell types including fibroblasts, myofibroblasts, and smooth muscle cells and is involved in vascular smooth muscle cell (VSMC) proliferation and tissue repair processes.[14–17] Immunostaining of whole mouse embryos at E15.5 revealed high levels of ACLP expression in collagen-rich tissues including the dermal layer of the skin, the medial layer of blood vessels, the basement membrane of the lung, and the periosteum.[16] We previously generated *Aebp1*$^{-/-}$ mice that develop spontaneous skin ulcerations and show delayed wound healing that corresponds with a reduction in dermal fibroblast proliferation.[16] In an experimental fibrosis model, *Aebp1*$^{-/-}$ mice also exhibit a decreased fibroproliferative response in the lung with reduced collagen deposition and myofibroblast accumulation.[15,18] Given the emerging role of *AEBP1* in ECM integrity, wound healing, and fibroproliferative pathways, it represents a highly plausible gene candidate for a human connective tissue disorder.

We performed molecular analyses on individuals who were referred to one of the collaborating academic centers for diagnostic workup of a suspected connective tissue disorder, but for whom previous genetic testing had been unrevealing. Each research subject provided written informed consent for sample collection and subsequent analysis under a protocol approved by one of the local institutional review boards. Blood samples were collected from the affected subjects as well as their unaffected parents. Skin biopsies were obtained from both affected subjects and unaffected family members when possible for fibroblast generation and subsequent analysis. To determine the molecular diagnosis in each subject, whole-exome sequencing (WES) was performed on genomic DNA extracted from blood leukocytes derived from the proband and parents in each family and run on different platforms. Details on the WES methodologies are available in the Supplemental Note. Sanger sequencing was used to confirm variants of interest in each subject and their relatives as well as the expected mode of inheritance.

Subject A-II:1 is a 35-year-old white male of German and Panamanian ancestry who was initially seen at the Mayo Clinic (Figures 1A–1E). Subject B-II:1 is a 36-year-old white male of Italian ancestry who was seen at the NIH (Figures 1F–1K and S2). Subjects C-IV:4 and C-IV:6 were seen at King Fahad Medical City in Saudi Arabia and have been reported previously.[9] The clinical phenotype in affected individuals exhibits significant clinical overlap with several EDS subtypes (classical [MIM: 130000], vascular [MIM: 130050], and arthrochalasia type [MIM: 130060]) and includes the presence of both major and minor supporting criteria including severe joint and skin laxity, osteoporosis affecting the hips and spine, osteoarthritis, soft redundant skin that can be acrogeria-like, delayed wound healing with abnormal atrophic scarring, and shoulder, hip, knee, and ankle dislocations (Figure 1 and Table 1). While the subjects described to date share many similarities, there are also variable features including gastrointestinal and genitourinary manifestations (bowel rupture, gut dysmotility, cryptorchidism, and hernias), vascular complications (mitral valve prolapse and aortic root dilation), and skeletal anomalies (Table 1). Significant clinical heterogeneity with a complex, multisystemic presentation is characteristic of other EDS subtypes, suggesting that the observed phenotypes are consistent with an EDS-spectrum disorder. Detailed clinical descriptions can be found within the Supplemental Note.

Exome sequencing of subject A-II:1 revealed compound heterozygous frameshift and nonsense variants in *AEBP1* comprising c.1470delC (chr7(GRCh37): g.44150393del; GenBank: NM_001129.4 for c.1470delC; GenBank: NP_001120.3 for p.Asn490Lysfs*6) in exon 12 and c.1743C>A (chr7(GRCh37): g.44151132C>A; GenBank: NM_001129.4 for c.1743C>A; GenBank: NP_001120.3 for p.Cys581*) in exon 15 (Figure 2). Testing of the subject's parents revealed that the c.1470delC variant was maternally inherited while the c.1743C>A variant was paternally inherited (Figure 1L). The c.1470delC variant was predicted to cause a frameshift mutation, denoted p.Asn490Lysfs*6. The c.1470delC variant was not observed in more than 123,136 exomes and 15,496 genomes in the Genome Aggregation Database (gnomAD).[19] The c.1743C>A (p.Cys581*) variant was seen in only one individual in gnomAD (1/264,694 alleles, MAF: 3.778×10^{-6}) (Table S1) and is predicted to cause loss of normal protein function either through protein truncation or nonsense-mediated decay. Exome sequencing of subject B-II:1 revealed a homozygous frameshift deletion variant in *AEBP1* in exon 11 (chr7(GRCh37): g.44149865_44149871del; GenBank: NM_001129.4 for c.1320_1326del; GenBank: NP_001120.3 for p.Arg440Serfs*3) (Figure 2). Sanger sequencing confirmed that both parents were carriers for the c.1320_1326del variant as well as an unaffected male sibling (Figure 1M). The variant was not observed in gnomAD (Table S1). Subjects C-IV:4 and C-IV:6 were previously found to have a homozygous splice site variant (chr7(GRCh37): g.44150657G>A; GenBank: NM_001129.4 for c.1630+1G>A) in intron 13 of *AEBP1* (Figure 2).[9] This variant has been observed in 9 individuals

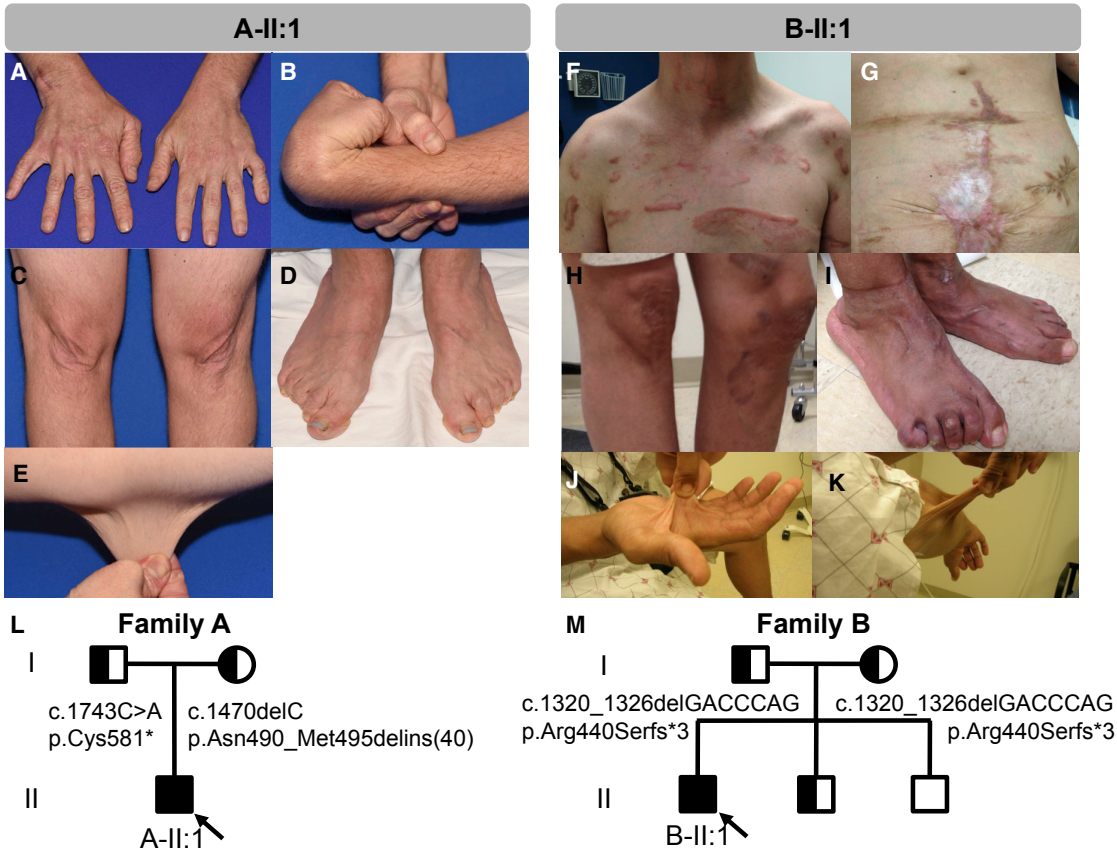

Figure 1. Clinical Features of Individuals with *AEBP1* Mutations

(A–E) Subject A-II:1 at the age of 31 exhibited (A, D) increased wrinkles on his hands and feet with finger contractures, (B) joint hypermobility with shoulder and hip subluxations, (C, E) excess stretchy skin, and (D) bilateral lesser hammertoe and hallux valgus deformities, pes planus, poor wound healing, and abnormal scarring.

(F–K) Subject B-II:1 was noted to have dislocated hip that required surgery, easy bruising, and dislocations of his shoulders. He has (F–H) severe abnormal scars that are widened, spread, hyperpigmented, and hypertrophic. At age 27 he presented with a ruptured bowel that was thought to be due to diverticulosis, and underwent repeated attempts to re-anastomose the bowel after which a colostomy bag was required (G). The subject has (I) severe pes planus with hammertoes and hallux valgus deformities as well as (J, K) hyperextensible soft skin.

(L) Family pedigree for subject A-II:1 shows that both parents are carriers for nonsense or truncating variants in *AEBP1*.

(M) Family pedigree for subject B-II:1 shows that both parents carry the same small deletion that results in premature truncation in *AEBP1*. The parents were not consanguineous, but did share some distant ancestry. Half-shaded symbols indicate carrier status and full shading indicates affected individuals in each family. Probands are indicated with arrows.

in gnomAD (9/271,654 individuals, no homozygotes, MAF: 3.313×10^{-5}). Sanger sequencing confirmed that one allele was inherited from their mother and the other from their father who are double first cousins.[9] No other clinically reportable variants were noted in any of the affected individuals, including in known connective tissue disorder genes.

RT-PCR analyses performed previously in individuals C-IV:4 and C-IV:6 showed that the c.1630+1G>A splice site variant results in the loss of the last 22 bp of exon 13 in *AEBP1*, resulting in a frameshift and truncation of the transcript.[9] To determine the functional consequence of the variants found in subjects A-II:1 and B-II:1, we compared *AEBP1* expression in dermal fibroblasts from the affected probands using RT-PCR and examined ACLP expression by western blotting as previously described.[16] In subject A-II:1, the c.1470delC variant was expected to induce a frameshift in the mRNA leading to an amino acid substitution at position 490 of the encoded protein followed by a stop codon after 6 amino acids (p.Asn490Lysfs*6). The c.1743C>A nonsense variant also generates a premature stop codon (p.Cys581*). Cell lysates from this individual, along with human U2OS and mouse 10T1/2 control cell lines, were examined by western blot analysis using an antibody against ACLP.[16] Unexpectedly, a band >170 kDa was detected in subject A-II:1, which was slightly larger than the band observed in either the U2OS and 10T1/2 controls (Figure 3A). To determine the nature of this protein, we isolated mRNA from these cells along with wild-type human dermal fibroblasts and generated cDNA which was amplified by PCR using primer sets that spanned both the c.1470delC and c.1743C>A variants. Interestingly, the PCR product spanning the c.1470delC variant was approximately 100 bp larger than

Table 1. Summary of Clinical Characteristics of Individuals with Autosomal-Recessive Mutations in *AEBP1*

	A-II:1	B-II:1	C-IV:6	C-IV:4
Citation	this report	this report	Alazami et al.[9]	Alazami et al.[9]
Sex	male	male	female	male
Ethnicity	white	white	Middle Eastern	Middle Eastern
Age at last evaluation	35 y	33 y	12 y	24 y
AEBP1 variant(s) (NM_001129.4)	c.1470delC; c.1743C>A; compound het	c.1320_1326del; homozygous	c.1630+1G>A; homozygous	c.1630+1G>A; homozygous
Protein change (NP_001120.3)	p.Asn490_Met495delins(40); p.Cys581*	p.Arg440Serfs*3	p.?	p.?
Beighton score	8 out of 9	8 out of 9	8 out of 9	unknown
Generalized joint hypermobility	+	+	+	+
Hip dislocation	hip subluxations reported	congenital hip dislocation, surgically corrected at 18 mo	dislocations reported	unknown
Shoulder dislocation	not reported	+	+	unknown
Foot deformities	pes planus, hallux valgus, hammer toes	pes planus, hallux valgus, hammer toes	pes planus, hallux valgus, hammer toes	pes planus, hallux valgus, toe deformities
Skin hyperextensibility	+	+	+	+
Excess skin/skin folding	increased wrinkles on hands and feet (acrogeria-like)	+	+	+
Delayed wound healing	+	+	+	+
Abnormal scarring	atrophic, widened scars	atrophic, widened scars with hyperpigmentation	hyperpigmented atrophic scars, multiple keloids	unknown
Easy bruising	+	+	+	unknown
Hernia	not reported	large ventral hernia developed at surgical sites secondary to ruptured bowel	umbilical, ventral, and inguinal	unknown
Genitourinary abnormalities	cryptorchidism, surgically corrected at 15 years of age	not reported	not reported	not reported
Gastrointestinal abnormalities	motility issues	bowel rupture	not reported	not reported
Vascular abnormalities	mitral valve prolapse	mitral valve prolapse, mildly dilated aortic root, bilateral stenosis of the carotids, aortic dilation requiring surgery	normal echo	normal echo
Dentition	retains a single baby tooth	not reported	abnormal dental alignment	unknown
Facial dysmorphisms	none	micrognathia	low posterior hairline, webbed neck, bilateral ptosis, excess redundant skin on face, large ears, narrow palate	unknown

(*Continued on next page*)

Table 1. *Continued*

	A-II:1	B-II:1	C-IV:6	C-IV:4
Skeletal anomalies	severe osteopenia involving the hips	hip replacement for severe osteopenia, upper thoracic scoliosis with degenerative disease and facet arthrosis of spine	skull shows 'copper beaten' appearance, severe osteopenia, narrowing of the interpedicular distance of the lumbar spines distally, iliac bones are short and squared, long bones of the lower extremities are remodeled	severe osteopenia
MRI findings	mild disc bulging at the C4-5 and C7-T1 levels	empty sella	not done	not done
Other	delays in walking and acquisition of fine motor skills, impaired temperature sensation, keratoconjunctivitis sicca, piezogenic papules on feet, right distal radioulnar joint dislocation, surgically repaired	elbow bursitis, piezogenic papules on feet, sacral dimple, and hypertriglyceridemia	uncontrolled diabetes mellitus, recurrent cellulitis	none

+ indicates clinical feature is present.

the wild-type sample (Figure 3B, indicated by an asterisk). This band was isolated and subjected to DNA sequencing. The expected single-nucleotide deletion was observed, but the cDNA fragment retained all 103 bp of intron 12 with in-frame continuation of exon 13 (Figure 3C). The predicted amino acid sequence derived from the mRNA sequence of the c.1470delC variant allele has loss of the last six amino acids encoded by exon 12 due to the shift in reading frame and inclusion of 40 aberrant amino acids before returning to the in-frame translation of exon 13, which we designated p.Asn490_Met495delins(40) (Figure 3D). Notably, this alteration occurs in the critical collagen-binding discoidin-like domain of ACLP, which we predict disrupts ACLP function. Similar studies were performed on fibroblasts derived from subject B-II:1. No ACLP protein was detected by western blot, suggesting that the homozygous c.1320_1326delGACCCAG variant identified in this individual leads to nonsense-mediated decay of the mRNA product and is a null variant (Figure 3E).

We next aimed to determine the functional consequence of ACLP loss in affected tissues derived from the research subjects. Ultrastructural examination of the skin, performed by transmission electron microscopy (TEM), revealed the presence of irregular disrupted collagen fibrils or "collagen flowers," with moderate variation in collagen size in subject A-II:1 (Figures 4A and 4B). Longitudinal sections revealed that these fibrils had a ragged or frayed appearance. Disrupted collagen fibrils can be found in several EDS variants and their presence can support a diagnosis of EDS but cannot differentiate between related subtypes. Trichome staining of skin derived from subject B-II:1 and examination under a light microscope revealed decreased dermal collagen when compared to heterozygous carriers and unaffected control subjects from the same family (Figures 4C–4E).

ACLP has several distinct domains that are thought to mediate different protein-protein interactions within the ECM. The central discoidin domain of ACLP shares significant homology and structural similarity with the discoidin domain-containing receptors (*DDR1* [MIM: 600408] and *DDR2* [MIM: 191311]). Within DDRs, the discoidin domain contains a collagen-binding region and helps mediate binding and specificity for fibrillar collagens, and pathogenic variants in *DDR2* are known to cause autosomal-recessive spondylometaepiphyseal dysplasia, short limb-hand type (SMED-SL [MIM: 271665]).[20–25] Knowing this, we expressed and purified a tagged ACLP discoidin domain and performed solid phase binding assays to determine the binding specificity across different fibrillar collagen types (Figure 5A). The purified recombinant discoidin domain was incubated with plastic coated with 10 μg/mL of either collagen I, II, III, IV, and V and fibronectin for 2 hr at room temperature. Binding was detected with primary anti-Xpress and secondary anti-mouse-HRP conjugated antibodies using a TMB substrate and absorbance measured at 450 nm. These studies revealed that the discoidin domain of ACLP binds to most collagens

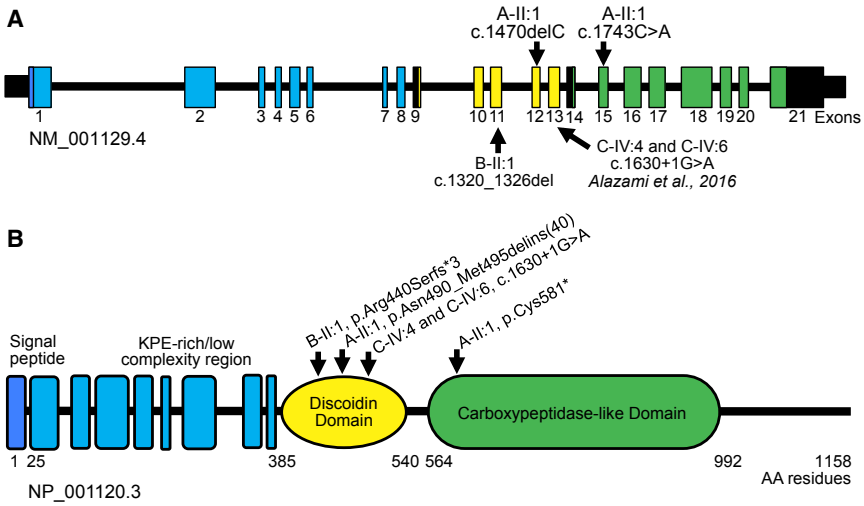

Figure 2. Schematic Representation of *AEBP1*, ACLP Protein Structure, and Summary of Known Mutations

(A) Exome sequencing revealed compound heterozygous (A-II:1) and homozygous (B-II:1) nonsense and small deletion frameshift variants in *AEBP1*. The homozygous splice site variant described in two siblings (C-IV:4 and C-IV:6) with similar clinical features by Alazami et al.[9] is also shown. *AEBP1* encodes the collagen binding protein.

(B) Aortic carboxypeptidase-like protein (ACLP) has several distinct domains that are thought to mediate different protein-protein interactions including a central discoidin domain that helps mediate binding and specificity for fibrillar collagens. ACLP also contains a catalytically inactive metallocarboxypeptidase-like domain. Mutations identified fell within the discoidin domain or immediately downstream and included nonsense, frameshift, and canonical splice site variants that were predicted to result in loss of function.

but has a preference for collagens I, III, and V which are mutated in other EDS subtypes (Figure 5A). Binding to collagen I was also shown to be dependent on glycosylation, with a reduction of binding to deglycosylated forms of collagen I (data not shown).

We then examined whether ACLP could promote collagen polymerization *in vitro*. Cell-free collagen polymerization assays using denatured collagen I generated an initial lag in absorbance at 410 nm followed by a sigmoidal rise in optical density and a slow linear rise or plateau (Figure 5B).[26] The sigmoidal part of the curve corresponds to the individual collagen molecules forming fibrils and the linear part of the curve corresponds to the total bundling of those fibrils. When full-length recombinant ACLP was added to the denatured collagen I, it significantly enhanced the collagen polymerization under physiological conditions (Figure 5B). These data suggest that ACLP is involved in organization and remodeling of the ECM through direct binding of collagens and modulation of collagen fibrillogenesis. Abnormal collagen fibril assembly in ACLP-deficient individuals could result in the observed EDS phenotypes and is supported by ultrastructural findings in the skin of affected individuals.

Through our studies we identified two individuals with bi-allelic pathogenic variants in *AEBP1* that encodes the collagen binding protein, ACLP, who are affected by a connective tissue disorder. The three variants in two unrelated families identified in this study, along with our previous report,[9] strongly support the notion that pathogenic variants in *AEBP1* result in a loss-of-function phenotype leading to connective tissue disease. We could not detect any ACLP protein in subject B-II:1 with the deletion variant predicted to cause a frameshift mutation (Figure 3E). Whether this results in the loss of mRNA by nonsense-mediated decay will require additional investigation. Unexpectedly, we did observe a protein product in subject A-II:1 (Figure 3A). Analysis of the mRNA indicated that this protein product is the result of the inclusion and translation of the intron between exons 12 and 13 (Figures 3B–3D). We could only very weakly detect mRNA product from the other allele by PCR (Figure 3B). We predict that the variants in family A result in loss of function via nonsense-mediated decay in one allele and a mutated and non-functional protein in the other allele. The central discoidin or factor V/VIII domain of ACLP is structurally similar to a number of proteins including those known to bind to collagens including the discoidin domain receptors.[12] Several diseases are caused by pathogenic variants in this highly conserved structural motif. For example, missense mutations in the discoidin domains of coagulation factor V and VIII cause factor V deficiency (MIM: 227400) and hemophilia A (MIM: 306700), respectively.[11] Mutations in the discoidin domain of retinoschisin cause X-linked juvenile retinoschisis (MIM: 312700) and several pathogenic variants result in changes in the number of cysteine residues reminiscent of the aberrantly expressed protein in subject A-II:1 (Figure 3B).[28]

ACLP is an ECM-associated protein that is highly expressed in collagen-rich tissues such as skin, the vasculature, and connective tissues,[14,16,17,29] and has roles in both embryonic development and adult tissue repair.[15–17] Fibroblasts lacking ACLP exhibit decreased contraction of collagen gels and this can be rescued through treatment with the exogenous ACLP discoidin domain or the full-length protein.[15] Mechanistically, ACLP modulates TGFβ1 receptor pathways to promote fibroblast to myofibroblast differentiation, which are processes necessary for wound repair.[18] *Aebp1*$^{-/-}$ mice develop spontaneous skin ulcerations and have significantly delayed healing of dermal punch wounds, which correlates with reduced dermal fibroblast proliferation *in vitro*.[16] This phenotype is reminiscent of the wound-healing defects and abnormal

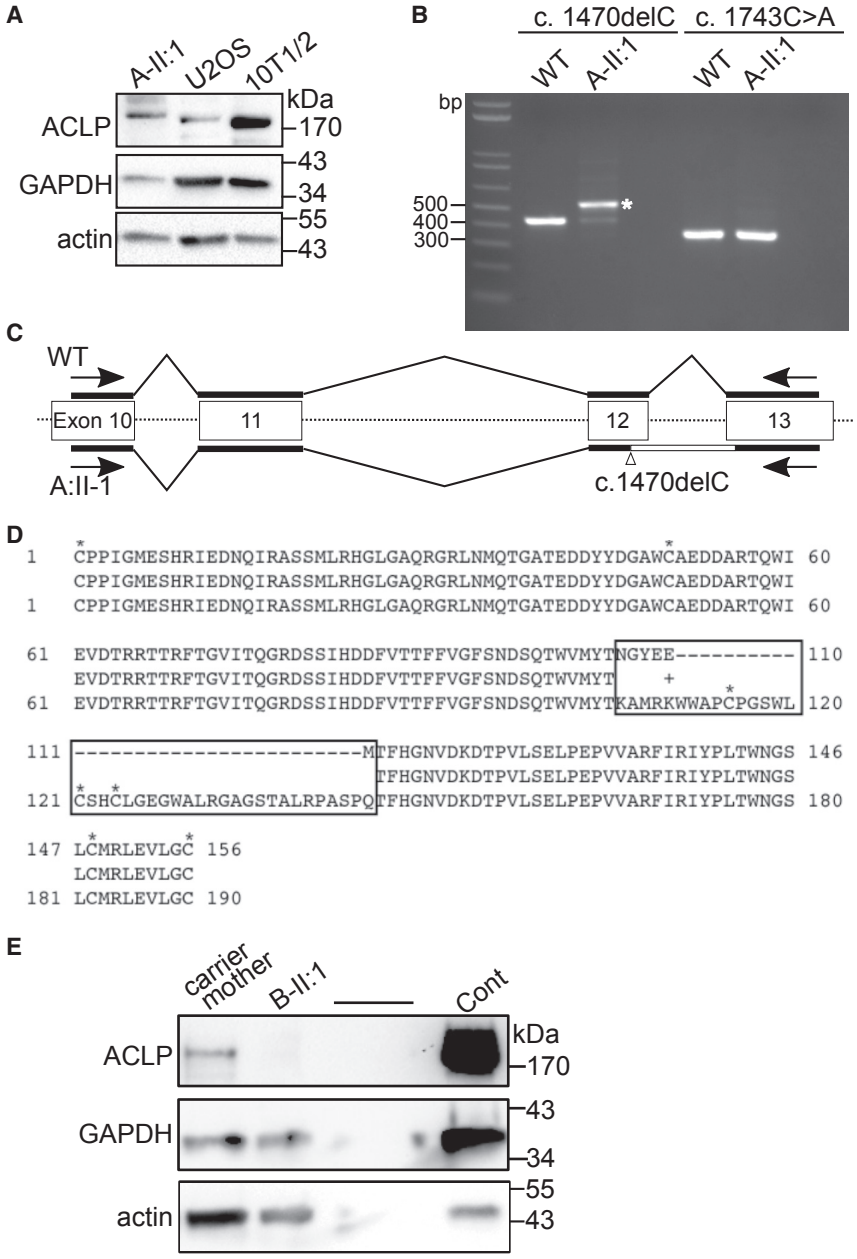

Figure 3. Analysis of *AEBP1* Mutant Fibroblast mRNA and Protein

Fibroblasts were isolated from dermal skin biopsies. Cells were routinely cultured in Dulbecco's Modified Eagle's Medium (Corning) with 3.7 g/L glucose, 10% fetal bovine serum (Hyclone), and 1% penicillin/streptomycin at 37°C in an 5% CO_2 incubator. Cells were passaged before they reached confluence using 0.25% trypsin/EDTA. All cells were genotyped by PCR of genomic DNA and sequencing prior to further analysis.

(A) Western blot analysis of protein lysates derived from fibroblasts from subject A-II:1. Anti-ACLP antibodies detected a band >170 kDa. Protein extracts were prepared as previously described[14,18] by washing the cells in cold PBS followed by extraction in 25 mM Tris (pH 7.4), 50 mM sodium chloride, 0.5% sodium deoxycholate, 2% NP-40, and 0.2% sodium dodecyl sulfate (SDS) with 1× Complete protease inhibitors cocktail (Roche) and 1× PhosStop phosphatase inhibitors cocktail (Roche). Lysates were incubated on ice for 15 min and cleared by centrifugation at 12,000 × *g* for 10 min at 4°C. The supernatant was collected and protein concentration was measured using the BCA kit (Thermo Scientific). Protein aliquots were run on 4%–20% Novex SDS-polyacrylamide gels and transferred to nitrocellulose. Blots were probed with antibodies against ACLP[14] and normalized to GAPDH (Sigma G9545, 1:10,000) and pan-actin (Thermo MS-1295B, 1:1,500).

(B) Fibroblasts were cultured in 12-well plates and total RNA was isolated and purified using GeneJET RNA Purification Kit (Thermo Scientific). cDNA was obtained using Maxima Reverse Transcriptase (Thermo Scientific). Regions of interest were amplified by PCR using OneTaq DNA polymerase (New England Biolabs) and the following primers: c.1470delC 5′-CCCATTGGGATGGAGTCACA-3′ (forward) 5′-CAGGTGAGTGGGTAGATGCG-3′ (reverse) producing a 422 bp product, and c.1743C>A 5′-GGCTCGTTTCATCCGCATCTA-3′ (forward) 5′-GCACCTCGTTGCCATGGAT-3′ (reverse) producing a 341 bp product. PCR products and controls were run on 2% agarose gels and bands of interest were purified using the QiaQuick Gel Extraction Kit (QIAGEN) followed by sequencing (Eton Bioscience). RNA was extracted from human ACLP-wild-type fibroblasts and from subject A-II:1, and following reverse transcription was amplified with PCR using primers spanning both genomic mutations. A band of approximately 520 bases was amplified (indicated by an asterisk).

(C) The DNA fragment (asterisk in B) was purified and subjected to DNA sequencing, which revealed that after the deletion in exon 12, the next intron was retained in the cDNA.

(D) The predicted amino acid sequence generated from the results of DNA sequencing and alignment with the wild-type sequence. The boxed region highlights different and additional amino acids, including the addition of three cysteines (indicated by an asterisk).

(E) Western blot analysis of protein lysates derived from fibroblasts from subject B-II:1 and his carrier mother with a murine fibroblast control.

scar formation observed in individuals with *AEBP1* deficiency and suggests that ACLP has a conserved role in damage sensing and ECM remodeling following injury.

Interestingly, the discoidin domain of ACLP preferentially binds collagens I, III, and V (Figure 5A). Of note, the clinical phenotypes observed in individuals with *AEBP1* mutations overlap with EDS subtypes caused by defects in these three collagen species (Table S2). ACLP also appears to play a role in collagen fibrillogenesis as suggested by the ultrastructural studies, which showed irregular disrupted collagen fibrils in dermal skin derived from one of the subjects described in this study. Consistent with this finding, we were able to show that ACLP promotes polymerization of collagen I *in vitro* (Figure 5B).

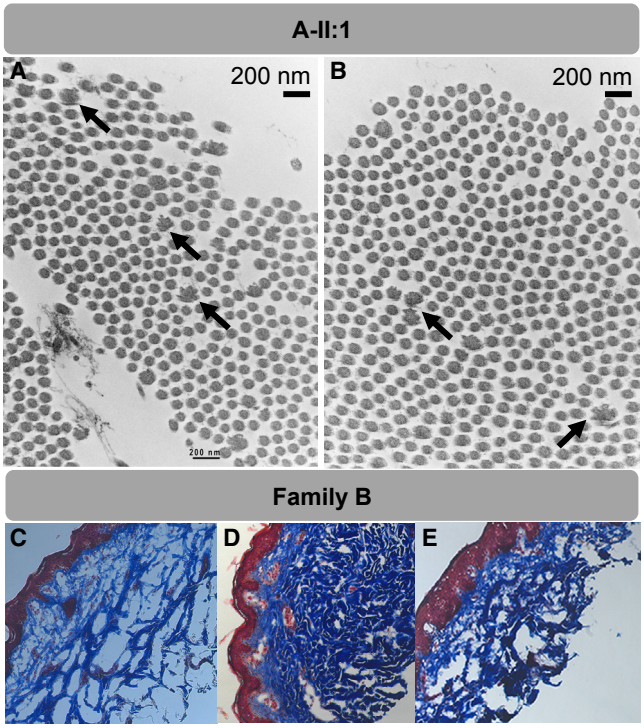

Figure 4. Ultrastructural and Histological Analysis of Skin Biopsies

For electron microscopy, skin biopsy specimens were fixed in glutaraldehyde, postfixed in osmium tetroxide, stained with uranyl acetate, and embedded in Spurr resin. Thin sections stained with lead citrate were examined on JEOL 1400 transmission electron microscope (JEOL USA).

(A and B) Collagen flowers identified by transmission election microscopy (TEM) in the proband in family A. Ultrathin sections of dermal collagen fibrils demonstrates moderate variation in fibril size and scattered composite collagen fibrils ("collagen flowers"); in longitudinal sections, these have a frayed/ragged moth-eaten appearance, and on cross sections, a flower-like appearance. Black arrows point to disordered collagen fibrils.

(C–E) Masson's trichrome staining of skin biopsies from family B show decreased dermal collagen in the proband. (C) B-II:1, the affected proband; (D) carrier brother; (E) carrier mother. Blue, dermis containing collagen bundles; red, epidermis. Original magnification, 100×.

Vascular smooth muscle cells in blood vessels have been shown to synthesize and secrete ACLP.[16] Aortic aneurysms (AAs) and aortic dissections are characterized by pathological remodeling of the aortic ECM.[30,31] In a recent study, ECM proteins and their degradation products were extracted from aneurysmal and control aortas which revealed increased expression as well as degradation of ACLP in the ECM of AAs.[30] Potentially related to these findings, echocardiography and MR angiography were performed in both individuals described in this study, which revealed mitral valve prolapse and evidence of aortic root aneurysm in one individual that required surgical intervention (see Supplemental Note). This individual also had a ruptured bowel at age 27 and developed large ventral hernias and severe scarring at the surgical site that was suggestive of vEDS (Figure 1, Supplemental Note). The major vascular complications in vEDS are aneurysms and dissection of the medium-sized arteries (renal, splenic, hepatic, etc.), but the aorta can be involved.[7] vEDS does not typically present with aneurysmal dilation of the ascending aorta at the sinuses of Valsalva, which is more commonly seen in Marfan (MIM: 154700) and Loeys-Dietz (LDS1 [MIM: 609192] and LDS2 [MIM: 610168]) syndromes (Table S2). Follow-up vascular surveillance was recommended in both individuals.

During embryonic development, ACLP is also highly expressed in bone, particularly in the periosteum,[29] and it is noteworthy that individuals with *AEBP1* mutations had osteoporosis affecting the hips and spine (Supplemental Note). The two individuals described in the study showed evidence of degenerative disc disease, facet arthrosis of spine, and osteoarthritis. A skeletal survey performed on the 12-year-old proband described previously revealed severe osteopenia, "copper beaten" skull, narrowing of the interpedicular distance of the lumbar spine distally, shortened and squared iliac bones, and remodeling of the long bones of the lower extremities (Figure S3). All the subjects had severe foot deformities including bilateral pes planus, hammertoes, and hallux valgus, which have been observed in other EDS subtypes. While the mechanisms for the bone changes in the ACLP-deficient individuals are unknown, a previous report detected *AEBP1* mRNA expression in an osteoblast cell line and its expression decreased with late calcification.[32] Further study will be required to examine the role of ACLP in bone development and homeostasis and its potential involvement in disorders of bone metabolism.

In summary, we have identified compound heterozygous and homozygous pathogenic variants in *AEBP1* in four affected individuals from three unrelated families to date. Affected individuals presented with a recognizable connective tissue disorder that falls in the EDS spectrum with joint hypermobility, skin laxity, delayed wound healing, abnormal scarring, aortic dilation, and osteoporosis. In addition, we show that the encoded protein, ACLP, is expressed within the skin, vasculature, and other connective tissues where it plays a critical role in ECM maintenance and tissue repair processes.

Supplemental Data

Supplemental Data include Supplemental Note (clinical reports), three figures, and two tables and can be found with this article online at https://doi.org/10.1016/j.ajhg.2018.02.018.

Acknowledgments

We would like to thank the subjects and their families for participating in this study. This work was made possible through support provided by the Mayo Clinic Center for Individualized Medicine (CIM) through the CIM Investigative and Functional Genomics Program. This work was supported by the Intramural Research Program of the National Institutes of Health, National Institute on Aging protocol numbers 03-AG-N330 (formerly 2003-086)

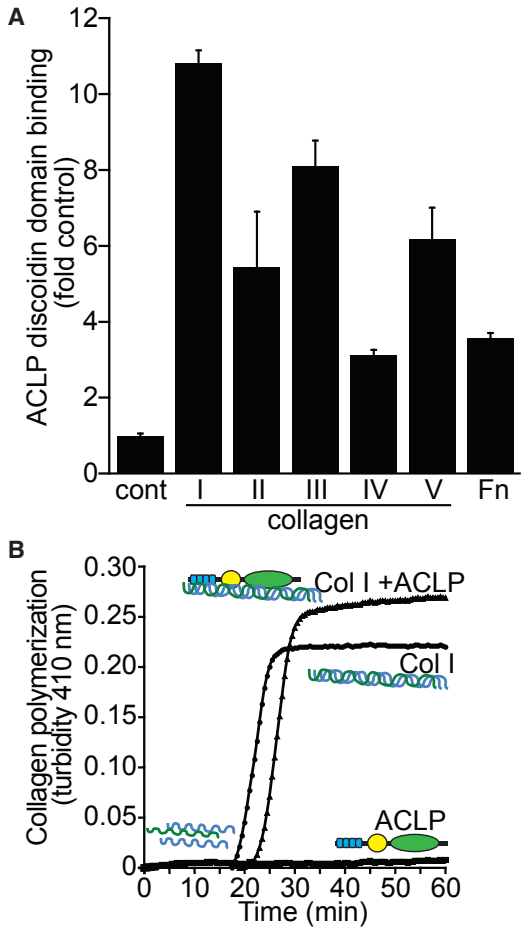

Figure 5. The Discoidin Domain of ACLP Binds to Fibrillar Collagens and Enhances Polymerization of Collagen I *In Vitro*

(A) Binding assays were performed as previously described.[21] Different extracellular matrix proteins were diluted to 10 μg/mL in PBS and each sample was coated to individual wells of a 96-well Corning cell culture plate overnight at room temperature. Proteins used were bovine gelatin (Sigma), rat collagen type I, bovine collagen type II, mouse type III collagen (Fibrogen), mouse collagen type IV, human collagen type V, and human fibronectin (BD Biosciences). Wells were washed with TBST (50 mM Tris [pH 7.4], 150 mM NaCl, 1% Tween-20) and blocked with 1 mg/mL casein (Sigma) in TBST for 1 hr followed by additional washes in TBST. Recombinant anti-Xpress tagged Discoidin-Like-Domain (DLD) protein was purified from BL21 bacteria as previously described.[15] Recombinant DLD binding assays were performed as above with coating of 10 μg/mL of extracellular matrix proteins to a 96-well Corning cell culture plate as described above. Wells were washed in TBST and blocked in 1 mg/mL casein in TBST for 1 hr followed by additional washes in TBST. DLD protein was diluted in TBST to 500 nM and was incubated with each extracellular matrix proteins for 2 hr at room temperature. Wells were washed 3× with TBST and anti-Xpress (Invitrogen) was diluted 1:1,000 in TBST then incubated with each sample for 1 hr. Additional TBST washes were performed and anti-mouse HRP was diluted 1:1,000 in TBST and incubated with each sample for 1 hr followed by washing. Signal was detected using the HRP substrate 3,3′,5,5′-tetramethylbenzidine (TMB) (eBiosciences) and reactions were stopped by the addition of 2 M H_2SO_4. Plates were read at OD 450 nm and results are presented as either fold control (plastic-only wells).

(B) Recombinant ACLP was generated as previously described.[18] In order to explore the role of ACLP in collagen fibril formation, a collagen polymerization assay was used.[26,27] Collagen I (0.6 mg/mL) was diluted in PBS containing 20 μg/mL rACLP and allowed to polymerize at 37°C for 1 hr in a clear 96-well plate. Readings at 410 nm were taken every 30 s using a BioTek Synergy HT system (Biotek). PBS containing only ACLP was also analyzed as a control.

and 11-AG-N079 (N.B.M. and C.A.F.), The American Heart Association grant 14GRNT18690001 (M.D.L.), and NIH grants HL078869 and HL078869S1 (M.D.L.). R.W.Z. was supported by a UROP award from Boston University. We acknowledge the support of the Saudi Human Genome Program.

Received: September 29, 2017
Accepted: February 20, 2018
Published: March 29, 2018

Web Resources

dbSNP, https://www.ncbi.nlm.nih.gov/projects/SNP/
ExAC Browser, http://exac.broadinstitute.org/
gnomAD Browser, http://gnomad.broadinstitute.org/
OMIM, http://www.omim.org/
Sequence Variant Nomenclature, http://varnomen.hgvs.org/
UniProt, http://www.uniprot.org/

References

1. Murphy-Ryan, M., Psychogios, A., and Lindor, N.M. (2010). Hereditary disorders of connective tissue: a guide to the emerging differential diagnosis. Genet. Med. *12*, 344–354.
2. Vanakker, O., Callewaert, B., Malfait, F., and Coucke, P. (2015). The genetics of soft connective tissue disorders. Annu. Rev. Genomics Hum. Genet. *16*, 229–255.
3. Byers, P.H., and Murray, M.L. (2012). Heritable collagen disorders: the paradigm of the Ehlers-Danlos syndrome. J. Invest. Dermatol. *132*, E6–E11.
4. Zou, Y., Donkervoort, S., Salo, A.M., Foley, A.R., Barnes, A.M., Hu, Y., Makareeva, E., Leach, M.E., Mohassel, P., Dastgir, J., et al. (2017). P4HA1 mutations cause a unique congenital disorder of connective tissue involving tendon, bone, muscle and the eye. Hum. Mol. Genet. *26*, 2207–2217.
5. Hynes, R.O., and Naba, A. (2012). Overview of the matrisome–an inventory of extracellular matrix constituents and functions. Cold Spring Harb. Perspect. Biol. *4*, a004903.
6. Mouw, J.K., Ou, G., and Weaver, V.M. (2014). Extracellular matrix assembly: a multiscale deconstruction. Nat. Rev. Mol. Cell Biol. *15*, 771–785.
7. Malfait, F., Francomano, C., Byers, P., Belmont, J., Berglund, B., Black, J., Bloom, L., Bowen, J.M., Brady, A.F., Burrows, N.P., et al. (2017). The 2017 international classification of the Ehlers-Danlos syndromes. Am. J. Med. Genet. C. Semin. Med. Genet. *175*, 8–26.
8. Beighton, P., De Paepe, A., Steinmann, B., Tsipouras, P., Wenstrup, R.J.; and Ehlers-Danlos National Foundation (USA) and Ehlers-Danlos Support Group (UK) (1998). Ehlers-Danlos syndromes: revised nosology, Villefranche, 1997. Am. J. Med. Genet. *77*, 31–37.
9. Alazami, A.M., Al-Qattan, S.M., Faqeih, E., Alhashem, A., Alshammari, M., Alzahrani, F., Al-Dosari, M.S., Patel, N., Alsagheir, A., Binabbas, B., et al. (2016). Expanding the clinical and genetic heterogeneity of hereditary disorders of connective tissue. Hum. Genet. *135*, 525–540.

10. Reznik, S.E., and Fricker, L.D. (2001). Carboxypeptidases from A to Z: implications in embryonic development and Wnt binding. Cell. Mol. Life Sci. *58*, 1790–1804.
11. Kiedzierska, A., Smietana, K., Czepczynska, H., and Otlewski, J. (2007). Structural similarities and functional diversity of eukaryotic discoidin-like domains. Biochim. Biophys. Acta *1774*, 1069–1078.
12. Carafoli, F., Bihan, D., Stathopoulos, S., Konitsiotis, A.D., Kvansakul, M., Farndale, R.W., Leitinger, B., and Hohenester, E. (2009). Crystallographic insight into collagen recognition by discoidin domain receptor 2. Structure *17*, 1573–1581.
13. Carafoli, F., Mayer, M.C., Shiraishi, K., Pecheva, M.A., Chan, L.Y., Nan, R., Leitinger, B., and Hohenester, E. (2012). Structure of the discoidin domain receptor 1 extracellular region bound to an inhibitory Fab fragment reveals features important for signaling. Structure *20*, 688–697.
14. Layne, M.D., Endege, W.O., Jain, M.K., Yet, S.F., Hsieh, C.M., Chin, M.T., Perrella, M.A., Blanar, M.A., Haber, E., and Lee, M.E. (1998). Aortic carboxypeptidase-like protein, a novel protein with discoidin and carboxypeptidase-like domains, is upregulated during vascular smooth muscle cell differentiation. J. Biol. Chem. *273*, 15654–15660.
15. Schissel, S.L., Dunsmore, S.E., Liu, X., Shine, R.W., Perrella, M.A., and Layne, M.D. (2009). Aortic carboxypeptidase-like protein is expressed in fibrotic human lung and its absence protects against bleomycin-induced lung fibrosis. Am. J. Pathol. *174*, 818–828.
16. Layne, M.D., Yet, S.F., Maemura, K., Hsieh, C.M., Bernfield, M., Perrella, M.A., and Lee, M.E. (2001). Impaired abdominal wall development and deficient wound healing in mice lacking aortic carboxypeptidase-like protein. Mol. Cell. Biol. *21*, 5256–5261.
17. Layne, M.D., Yet, S.-F., Maemura, K., Hsieh, C.M., Liu, X., Ith, B., Lee, M.E., and Perrella, M.A. (2002). Characterization of the mouse aortic carboxypeptidase-like protein promoter reveals activity in differentiated and dedifferentiated vascular smooth muscle cells. Circ. Res. *90*, 728–736.
18. Tumelty, K.E., Smith, B.D., Nugent, M.A., and Layne, M.D. (2014). Aortic carboxypeptidase-like protein (ACLP) enhances lung myofibroblast differentiation through transforming growth factor β receptor-dependent and -independent pathways. J. Biol. Chem. *289*, 2526–2536.
19. Lek, M., Karczewski, K.J., Minikel, E.V., Samocha, K.E., Banks, E., Fennell, T., O'Donnell-Luria, A.H., Ware, J.S., Hill, A.J., Cummings, B.B., et al.; Exome Aggregation Consortium (2016). Analysis of protein-coding genetic variation in 60,706 humans. Nature *536*, 285–291.
20. Curat, C.A., Eck, M., Dervillez, X., and Vogel, W.F. (2001). Mapping of epitopes in discoidin domain receptor 1 critical for collagen binding. J. Biol. Chem. *276*, 45952–45958.
21. Leitinger, B. (2003). Molecular analysis of collagen binding by the human discoidin domain receptors, DDR1 and DDR2. Identification of collagen binding sites in DDR2. J. Biol. Chem. *278*, 16761–16769.
22. Abdulhussein, R., McFadden, C., Fuentes-Prior, P., and Vogel, W.F. (2004). Exploring the collagen-binding site of the DDR1 tyrosine kinase receptor. J. Biol. Chem. *279*, 31462–31470.
23. Xu, H., Raynal, N., Stathopoulos, S., Myllyharju, J., Farndale, R.W., and Leitinger, B. (2011). Collagen binding specificity of the discoidin domain receptors: binding sites on collagens II and III and molecular determinants for collagen IV recognition by DDR1. Matrix Biol. *30*, 16–26.
24. Fu, H.-L., Valiathan, R.R., Arkwright, R., Sohail, A., Mihai, C., Kumarasiri, M., Mahasenan, K.V., Mobashery, S., Huang, P., Agarwal, G., and Fridman, R. (2013). Discoidin domain receptors: unique receptor tyrosine kinases in collagen-mediated signaling. J. Biol. Chem. *288*, 7430–7437.
25. Bargal, R., Cormier-Daire, V., Ben-Neriah, Z., Le Merrer, M., Sosna, J., Melki, J., Zangen, D.H., Smithson, S.F., Borochowitz, Z., Belostotsky, R., and Raas-Rothschild, A. (2009). Mutations in DDR2 gene cause SMED with short limbs and abnormal calcifications. Am. J. Hum. Genet. *84*, 80–84.
26. Damodarasamy, M., Vernon, R.B., Karres, N., Chang, C.H., Bianchi-Frias, D., Nelson, P.S., and Reed, M.J. (2010). Collagen extracts derived from young and aged mice demonstrate different structural properties and cellular effects in three-dimensional gels. J. Gerontol. A Biol. Sci. Med. Sci. *65*, 209–218.
27. Silver, F.H., and Birk, D.E. (1983). Kinetic analysis of collagen fibrillogenesis: I. Use of turbidity–time data. Coll. Relat. Res. *3*, 393–405.
28. Dunnen, J.T., Kraayenbrink, T., Van Schooneveld, M., Van Vosse, E.D., De Jong, P.T.V.M.; and The Retinoschisis Consortium (1998). Functional implications of the spectrum of mutations found in 234 cases with X-linked juvenile retinoschisis. Hum. Mol. Genet. *7*, 1185–1192.
29. Ith, B., Wei, J., Yet, S.-F., Perrella, M.A., and Layne, M.D. (2005). Aortic carboxypeptidase-like protein is expressed in collagen-rich tissues during mouse embryonic development. Gene Expr. Patterns *5*, 533–537.
30. Didangelos, A., Yin, X., Mandal, K., Saje, A., Smith, A., Xu, Q., Jahangiri, M., and Mayr, M. (2011). Extracellular matrix composition and remodeling in human abdominal aortic aneurysms: a proteomics approach. Mol. Cell. Proteomics *10*, 008128.
31. Pepin, M.G., Schwarze, U., Rice, K.M., Liu, M., Leistritz, D., and Byers, P.H. (2014). Survival is affected by mutation type and molecular mechanism in vascular Ehlers-Danlos syndrome (EDS type IV). Genet. Med. *16*, 881–888.
32. Ohno, I., Hashimoto, J., Shimizu, K., Takaoka, K., Ochi, T., Matsubara, K., and Okubo, K. (1996). A cDNA cloning of human AEBP1 from primary cultured osteoblasts and its expression in a differentiating osteoblastic cell line. Biochem. Biophys. Res. Commun. *228*, 411–414.

The American Journal of Human Genetics, Volume *102*

Supplemental Data

Bi-allelic Alterations in *AEBP1* Lead to Defective Collagen Assembly and Connective Tissue Structure Resulting in a Variant of Ehlers-Danlos Syndrome

Patrick R. Blackburn, Zhi Xu, Kathleen E. Tumelty, Rose W. Zhao, William J. Monis, Kimberly G. Harris, Jennifer M. Gass, Margot A. Cousin, Nicole J. Boczek, Mario V. Mitkov, Mark A. Cappel, Clair A. Francomano, Joseph E. Parisi, Eric W. Klee, Eissa Faqeih, Fowzan S. Alkuraya, Matthew D. Layne, Nazli B. McDonnell, and Paldeep S. Atwal

Supplemental Note

Case Reports

Subject A-II:1 is a 35-year-old white male of German and Panamanian ancestry who has been followed from a young age. He exhibited a complicated history of preterm birth and was noted to have several congenital abnormalities including cryptorchidism that was repaired at age 15, redundant skin, and joint laxity. He also reported delays in walking and difficulty with fine motor skills in his left hand. On recent examination, this individual was found to have normal motor function with no focal deficits. The subject exhibited increased wrinkles on his hands and feet, right shoulder and hip subluxations, hammertoes, chronic constipation, impaired temperature sensation, poor wound healing, and abnormal bleeding (Figure 1A-E). The subject was diagnosed with EDS at 15 years of age and previous genetic testing for variants in collagen genes was unrevealing.

A workup revealed no kyphoscoliosis or hernias, negative Gorlin sign, and normal colored sclera with possible keratoconus present. The subject's palms were hyperlinear and atrophic and the dorsal sides were atrophic, hyperlinear, and extensible (Figure 1). He has extremely extensible skin with retained elasticity at the elbows; his knees also exhibited extremely extensible skin with subtle laxity and redundancy noted when the knee was in the extended position (Figure 1). He has widened fishmouth-like atrophic scars on his left knee and back, pes planus, and piezogenic papules on his feet. The subject had a Beighton score of 8 out of 9.

The subject had a history of syncope in his youth and has intermittent palpitations particularly at night. He was found to have mitral valve prolapse on a previous evaluation. A vascular workup, which included magnetic resonance angiography (MRA) of the head, neck, and chest, revealed no evidence of stenosis, aneurysm, or dissection and normal vascular architecture with the exception of the left vertebral artery, which is diffusely small in caliber developmentally. There were no other similarly affected individuals in the subject's family (Figure 1L). Currently, he has no history of hypertension, hyperlipidemia, or diabetes.

X-ray examination of the spine showed straightening of the normal lumbar lordotic curve with lower lumbar facet arthrosis with minimal disc space narrowing and retrolisthesis L5-S1. There was also mild disc space narrowing L4-L5. The remaining disc spaces were preserved. There was proliferative degenerative wedging at the thoracolumbar junction. There was mild disc space narrowing and anterior subluxation at C5-C6 with similar changes at C6-C7. There was also lower cervical facet arthrosis with slight anterior subluxation and disc space narrowing at C7-T1. No fractures were observed.

Dual-energy X-ray absorptiometry (Lunar iDXA) revealed a hip bone mineral density that fell significantly below the expected range for the subject's age, consistent with osteoporosis (Figure S1). Total BMD for left hip is 0.781 g/cm^2,

with T-Score of -1.8 and Z-Score of -2.1; total BMD for right hip is 0.789 g/cm^2, with T-Score of -1.7 and Z-Score of -2.0; total BMD for left femoral neck is 0.816 g/cm2, with a T-Score -1.6 and Z-Score of -1.8; total BMD for right femoral neck is 0.884 g/cm^2, with a T-Score -1.1 and Z-Score of -1.3.

Whole exome sequencing was performed by GeneDx (Gaithersburg, MD) using the Agilent Clinical Research Exome kit to target the exonic regions and flanking splice junctions of the genome. These targeted regions were sequenced on an Illumina HiSeq 2000 sequencing system with 100 bp paired-end reads. Bi-directional sequence was assembled, aligned to reference gene sequences based on human genome build GRCh37/UCSC hg19, and analyzed for sequence variants using a custom-developed analysis tool (Xome Analyzer). Capillary sequencing or another appropriate method was used to confirm all potentially pathogenic variants identified in this individual and their relatives. Sequence alterations were reported according to the Human Genome Variation Society (HGVS) nomenclature guidelines. The exome was covered to a mean depth of 121x, with a quality threshold of 94.3%.

Subject B-II:1 is a 41-year-old white male of Italian ancestry who had been followed since birth for congenital hip dislocation, easy bruising, and repeat dislocation of his shoulders. He had surgical correction at 18 months for dislocated hip, which healed with a large scar (Figure S2). The subject's scars are unusual and appear widened, spread, hyperpigmented, and atrophic (Figure

1). He developed elbow bursitis at the age of 21, which required surgical evacuation. At 27 years of age he was hospitalized for ruptured bowel, which was thought to be due to diverticulosis. The surgeon noted abnormal tissue during the procedure and repeated attempts to re-anastomose the bowel failed and a colostomy was required (Figure 1G). A large ventral hernia developed at one of the surgical sites and severe scarring was apparent. The subject later had his colostomy reversed and ventral hernia closed. Additionally, the subject has micrognathia, downsloping shoulders, soft, hyperextensible skin, piezogenic papules on his feet, severe pes planus, sacral dimple, and hypertriglyceridemia (Table 1). When the subject presented to medical genetics, vascular-type EDS was considered based on the presence of hollow organ rupture, impaired wound healing, abnormal scaring, and joint dislocations. The subject had a Beighton score of 8 out of 9. Sequencing analysis and deletion/duplication studies of *COL3A1* revealed no variants in this gene. The subject's family does not have a history of connective tissue disease (Figure 1M).

When this individual was 32 years of age, he had an echocardiogram that showed a hyperdynamic left ventricle that was normal in size with an estimated ejection fraction of 65-70%. The right ventricle was normal. The mitral valve was normal in structure and function but had a slight focal prolapse posterior leaflet with mild mitral regurgitation. The tricuspid valve was normal with trace regurgitation. Measurements of the great vessels showed an aortic annulus

measuring 2.2 cm, the sinuses of Valsalva measuring 3.8 cm, the sino-tubular junction measuring 3.8 cm and the ascending aorta measuring 3.6 cm.

A repeat echo at 36 years of age showed aortic root dilation with other parameters largely unchanged from the previous exam. Measurements of the great vessels showed an aortic annulus measuring 2.3 cm, the sinuses of Valsalva measuring 4.0 cm, the sino-tubular junction measuring 2.6 cm and the ascending aorta measuring 3.1 cm. The aortic root diameter was calculated to be 4.0 cm.

Contrast MRA was also performed on this individual at this time and confirmed a dilated aortic root measuring 4.2 cm. The descending aorta was normal in size and the aortic artery was unremarkable as was the descending thoracic aorta. The abdominal aorta including the celiac artery, superior mesenteric artery, and a separate common hepatic artery between the celiac and superior mesenteric artery were normal with no evidence of aortic aneurysm. These measurements are indicative of aortic dilation. Correspondence with this individual after the NIH study was closed revealed that his aortic root had dilated further and surgery was required.

MRI of the brain and spine revealed an empty sella as well as upper thoracic scoliosis with degenerative disease and facet arthrosis of spine. Dual-energy X-ray absorptiometry at 36 years of age showed a hip BMD that fell below the

expected range for this individual's age, consistent with osteoporosis. His total BMD was 1.002 g/cm^2 with a T-Score -2.7 and Z-Score of -2.1. Total BMD for left hip was 0.747 g/cm^2, with T-Score of -2.5 and Z-Score of -2.0; total BMD for right hip was 1.059 g/cm^2, with T-Score of -0.3 and Z-Score of 0.2; total BMD for left femoral neck is 0.808 g/cm^2, with a T-Score -2.0 and Z-Score of -1.5; total BMD for right femoral neck is 1.135 g/cm^2, with a T-Score 0.5 and Z-Score of 1.0. He later developed severe degenerative disease of the hips requiring hip replacement.

Genomic DNA was extracted from whole blood collected from subject B-II:1 and both parents and was fragmented and subjected to whole-exome capture with the SureSelect Human All Exon 50Mb kit (Agilent Technologies) following the manufacturer's protocols. Exome capture libraries were then sequenced on the Illumina HiSeq 2000 platform according to the manufacturer's instructions, and 100-bp paired-end reads were generated. Sequencing and subsequent analysis including alignment and variant calling were performed at the Beijing Genomics Institute (BGI Inc., Shenzhen, China). Potentially pathogenic variants were confirmed by Sanger sequencing on the ABI Genetic Analyzer 3130xl (Applied Biosystems, Foster City, CA). Absence of variants in *COL3A1*, *COL5A1* and *PLOD1* was confirmed by Sanger sequencing and multiplex ligation-dependent probe amplification (MLPA) using probes set P155 (EDS probemix, MRC-Holland, Amsterdam, Netherlands).

Subject C-IV:6 initially described in Alazami et al. (Family 1 ID: 14DG1601) was born post-term by C-section at 42 weeks gestation with a birth weight of 4.3 kg. She was admitted to intensive care because of hypotonia and poor feeding and was noted to have severe joint and skin laxity and talipes deformity. She had delayed motor milestones that improved with age. She walked at 20 months but attained speech at an appropriate age. There is family consanguinity with parents being double 1st cousins with 7 siblings; one brother (IV:4) manifested with similar features which were diagnosed as myopathy of unknown etiology. Genetic testing showed that he was also homozygous for the c.1630+1G>A splice site variant in *AEBP1*.

At 10 years of age the subject had a weight of 62 kg (>95th percentile), height of 142.5 cm (75th percentile), and OFC of 50 cm (~25th percentile). She had coarse facial features as well as severe skin and joint laxity. There was a generalized skin redundancy with sagging cheeks, micrognathia with high arched palate and gross dental misalignments, bilateral ptosis with thinning of the eyebrows. The neck was short and webbed with low hairline and large ears. The phenotype of the small and large joints included dislocations involving the hips, knees, ankles, and interphalangeal (IP) joints. She also had multiple variable-sized keloids.

Skeletal survey showed severe osteopenia, both fore feet were abducted, and hind feet were in valgus position. There was lateral subluxation of middle

interphalangeal joint of the 2nd toe. There is bilateral hallux valgus and distal narrowing of the interpedicular distance. The iliac bone also had a squared appearance. Abdominal US showed hepatomegaly with severely contracted gallbladder.

Supplemental Figures

Supplemental Figure 1. Bone densitometry and partial skeletal survey of subject A-II:1

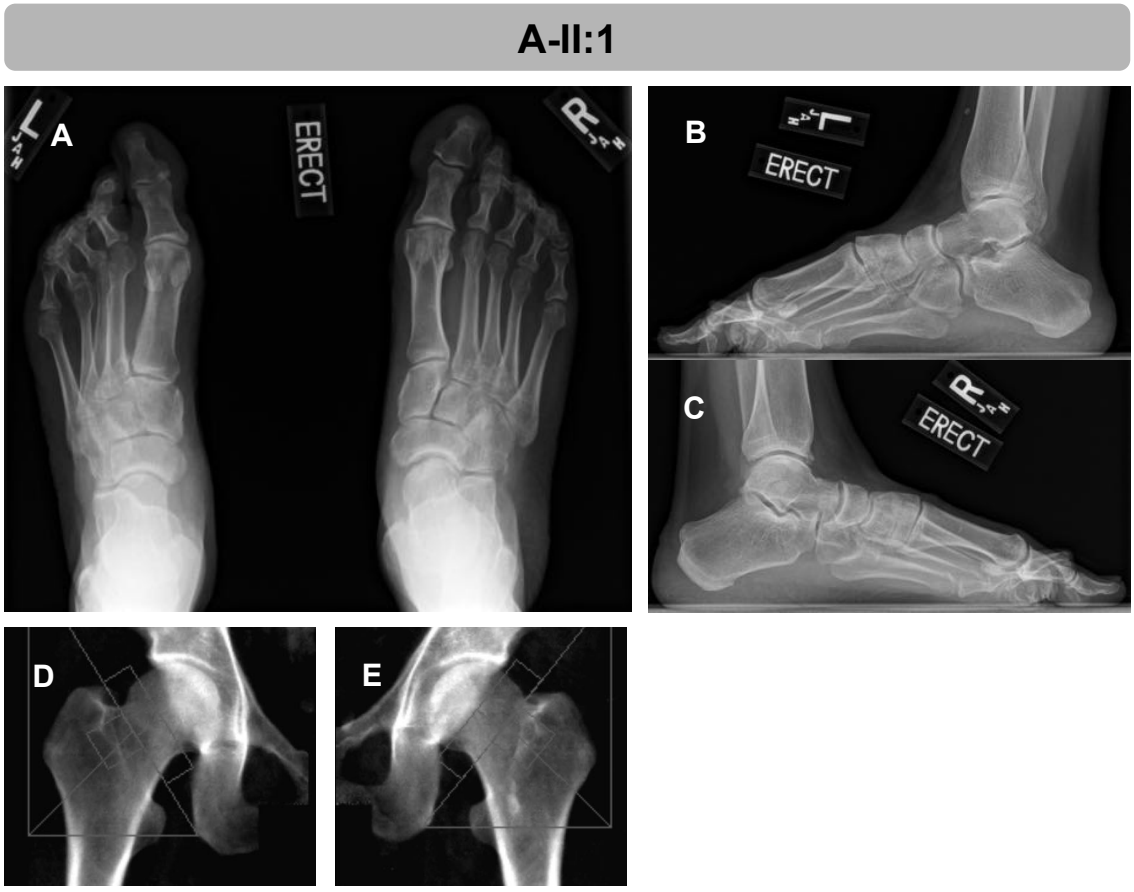

(A-C) Standing X-rays of left and right foot. This individual was noted to have bilateral lesser hammertoe and hallux valgus deformities. Moderate bilateral great toe metatarsophalangeal joint osteoarthritis, right greater than left was also

noted with diffuse mild osteoarthritis throughout both mid feet and forefeet. An osteochondral lesion of the right talar head can be seen on the dorsal plantar radiograph. (D,E) Dual-energy X-ray absorptiometry (Lunar iDXA) revealed a hip bone mineral density (BMD) that fell below the expected range for this individual's age, consistent with osteoporosis.

Figure S2. Additional photographs of subject B-II:1

The subject had poor wound healing with atrophic scars that were both widened and hyperpigmented. (A) Widened atropic scar from hip surgery at 18 months for

dislocated hip. (B) Abnormal surgical scar from repair of a ruptured bowel at 27 years of age. Repeated attempts to re-anastomose the bowel failed and a colostomy was required. A large ventral hernia later developed and was repaired and the colostomy reversed. (C) Piezogenic papules were present bilaterally. (D) Abnormal keloid scars on the chest with bruises apparent. (E,F) Papyraceous scars at both the elbows and knees. (G,H) The skin on the chest and abdomen was translucent with veins visible beneath the skin. Multiple abnormal scars were also present, some with a keloid appearance.

Figure S3. Skeletal survey of 12-year-old proband C-IV:6

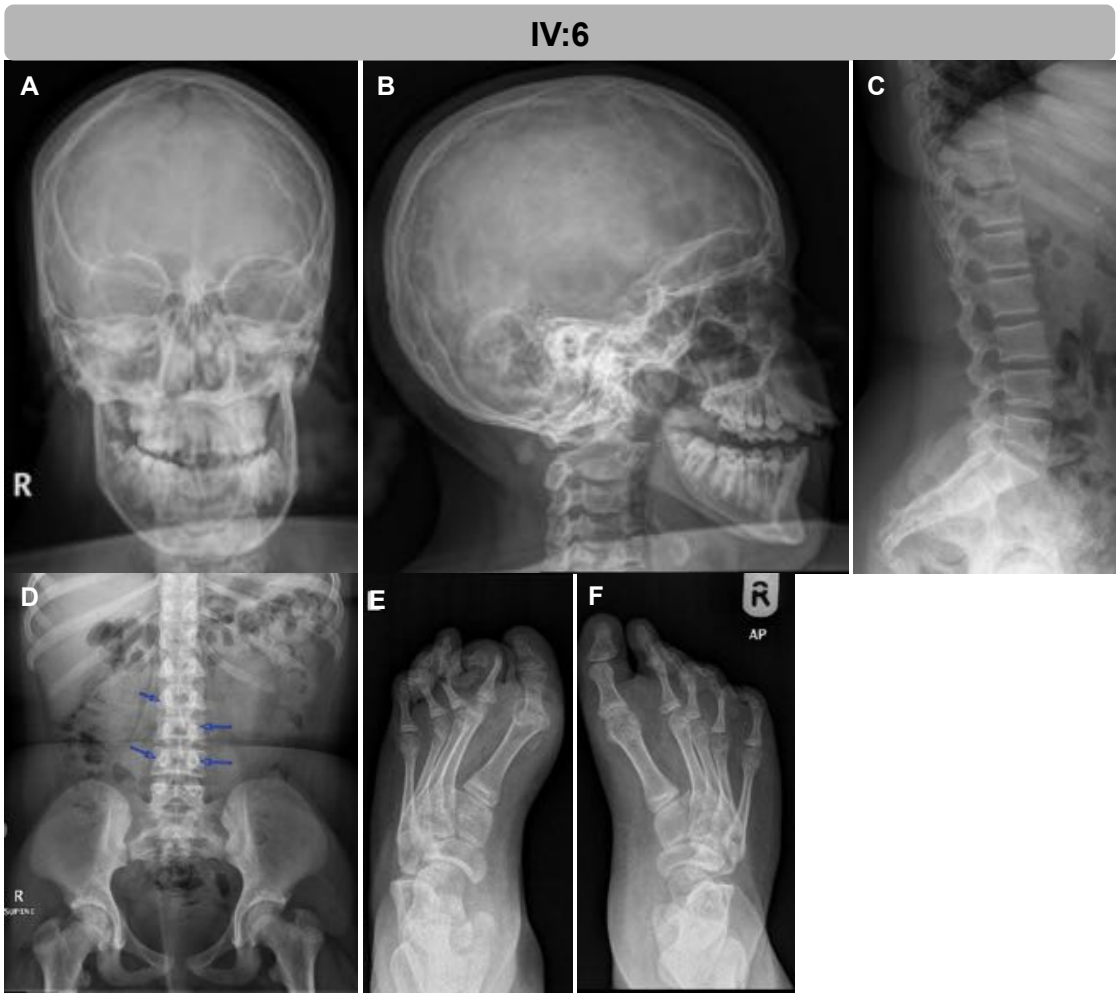

(A,B) Posteroanterior and lateral views of the skull showing 'copper beaten' appearance of the cranium and abnormal dental alignment. (C,D) Lumbar spine lateral and anteroposterior projection. The alignment of the spine is unremarkable, however narrowing of the interpedicular distance of the lumbar spines distally was observed. The iliac bones were also shortened and squared. There is no acetabular dysplasia or femoral head dislocation. (E,F) Standing X-rays of left and right foot showed bilateral lesser hammertoe and hallux valgus deformities.

Supplemental Tables

Table S1. Summary of *AEBP1* variant findings in each individual.

Subject	gDNA (GRCh37/hg19)	Exon	Transcript cDNA NM_001129.4	Coding Effect	Protein Change	Zygosity	gnomAD Allele Frequency	dbSNP	Reference
A-II:1	Chr7:44150393del	12	c.1470delC	Frameshift	p.Asn490_Met495 delins(40)	Het	N/R	N/R	This report
A-II:1	Chr7:44151132C>A	15	c.1743C>A	Nonsense SNV	p.Cys581*	Het	1/264694	rs777647845	This report
B-II:1	Chr7:44149865_44 149871del	11	c.1320_1326del	Frameshift	p.Arg440Serfs*3	Hom	N/R	N/R	This report
C-IV:4 and C-IV:6	Chr7:44150657G>A	13	c.1630+1G>A	Abolishes splice donor	p.?	Hom	9/271654	rs369016031	Alazami et al., 2016

Het, heterozygous; hom, homozygous; N/R, not reported.

Table S2. Comparison of *AEBP1*-related clinical phenotypes with EDS subtypes in the updated 2017 International Classification Guidelines.